
AUTHOR QUERIES

Journal id: TPHM_A_407650

Corresponding author: Xiaobing Ren

Title: Strain glass in ferroelastic systems: premartensitic tweed versus strain glass

Dear Author

Please address all the numbered queries on this page which are clearly identified on the proof for your convenience.

Thank you for your cooperation

Query number	Query
-----------------	-------

IF POSSIBLE, PLEASE ENSURE THAT CONSTANTS, VARIABLES, UNITS, ETC. IN FIGURE ARTWORK CORRESPOND WITH THOSE IN TEXT. NOTE ITALICS IN ARTWORK: TG, T (K), X, XC, ETC., EMU/GM → EMU/G, ALSO SPACING BETWEEN AMOUNTS AND UNITS.

- | | |
|---|--|
| 1 | Please update references [28] and [29] and provide full author names |
|---|--|
-

Strain glass in ferroelastic systems: premartensitic tweed versus strain glass

Xiaobing Ren^{ab*}, Yu Wang^{ab}, Yumei Zhou^{ab}, Zhen Zhang^{ab}, Dong Wang^a,
Genlian Fan^{ab}, Kazuhiro Otsuka^{ab}, Tetsuro Suzuki^{ab}, Yuanchao Ji^b,
5 Jian Zhang^b, Ya Tian^b, Sen Hou^b and Xiangdong Ding^b

^a*Ferroc Physics Group, National Institute for Materials Science, Tsukuba 305-0047, Japan;* ^b*Multi-Disciplinary Materials Research Center, Xi'an Jiaotong University, Xi'an 710049, China*

(Received 28 March 2009; final version received 9 November 2009)

10 Cluster-spin glass and ferroelectric relaxor have been observed in defect-
containing ferromagnetic systems and ferroelectric systems, respectively.
However, it is unclear whether or not an analogous glass state exists in
the physically parallel ferroelastic (or martensitic) systems. In the 1990s,
15 theoretical studies suggested that premartensitic tweed can be viewed as
a strain glass. However, there has been no experimental verification of this
hypothesis. In this paper, we provide an experimental test of this hypothesis
by measuring the possible glass signatures in two well-known premar-
tensitic tweed systems prior to their martensitic transformation: one
20 $\text{Ni}_{63}\text{Al}_{37}$ and the other $\text{Ti}_{50}\text{Ni}_{47}\text{Fe}_3$ martensitic alloy. Our experiments
show that no glass signatures exist for the premartensitic tweed in both
systems. There is no mechanical susceptibility/modulus anomaly in the
tweed temperature regime, suggesting no glass transition exists. The tweed
remains ergodic, inconsistent with a frozen glass. These two critical
25 experiments show that premartensitic tweed is not a frozen glass state.
We demonstrate that strain glass exists in ferroelastic/martensitic systems
but only in defect-containing ferroelastic/martensitic systems with defect
concentration exceeding a critical value. This strain glass is a mechanical
analogue of cluster-spin glass or ferroelectric relaxor, and possesses all
30 the features of a glass. We further show that the tweed is equivalent to
an ‘unfrozen state’ of a strain glass. Finally, we demonstrate that the
microscopic origin of the strain glass can be easily understood in analogy
with the behavior of a ‘defect-containing domino array’.

Keywords: strain glass; tweed; precursor effect; glass transition; martensitic
transformations; phase transitions

35 1. Introduction

All matter tends to take a more ordered form at low temperature to reduce entropy
as required by the third law of thermodynamics [1]. This thermodynamic require-
ment is the origin of a variety of disorder to order transitions observed in nature.
The most familiar example is the liquid to crystal transition, which is an ordering of

*Corresponding author. Email: ren.xiaobing@nims.go.jp

40 atomic configuration. Ordering of other physical quantities is also well known,
such as the ordering of magnetic moment, electric dipole or lattice strain. The
corresponding disorder–order transitions are ferromagnetic transition, ferroelectric
transition and ferroelastic/martensitic transition, respectively. These transitions
play a central role in structural and functional materials and are also an important
45 subject in materials science and physics [2].

Contrary to the above disorder–order transitions, which are driven by a thermo-
dynamic requirement to reduce entropy, there exists another large class of transitions
– the ‘glass transitions’, where a disordered state is frozen into a statically disordered
phase with local order only [3]. As the disordered glass state is not a favorable
50 low temperature state (i.e. low entropy state) from a thermodynamic point of view,
disorder–glass transition is not a thermodynamic transition and cannot be explained
from thermodynamic principles.

Disorder–glass transitions are conjugate transitions of their corresponding
disorder–order transitions, as shown in Figure 1. They are often formed by doping
55 point defects into a system showing normal disorder–order transition. The most
familiar disorder–glass transition is structural glass transition, which is the conjugate
transition of liquid to crystal. Structural glass transition can be formed by doping
a sufficient amount of point defects (or dopants) into a pure system that has
a normal liquid to crystal transition. A common example is where dissolving gelatin
60 in water suppresses the crystallization transition (ice formation) and, instead,
the gelatin water transforms into a structural glass (the jelly!). Similarly, ferromagnetic

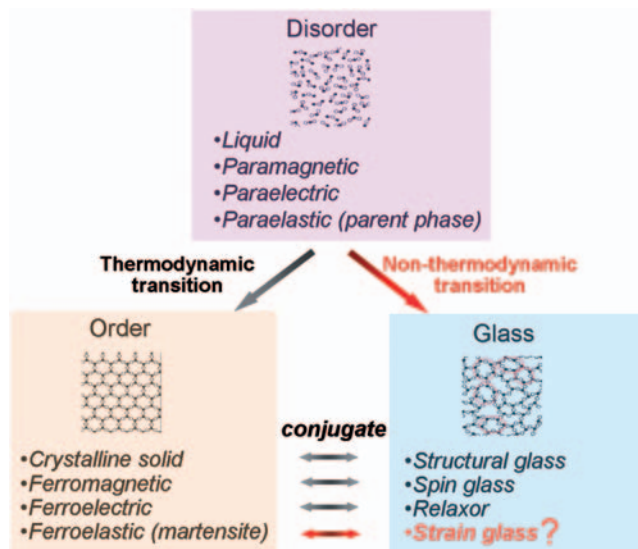


Figure 1. Two classes of phase transitions in nature: disorder–order and disorder–glass (frozen disorder). A glass transition can be viewed as a conjugate transition of a corresponding disorder–order transition. Strain glass is expected because a conjugate glass transition of a ferroelastic (or martensitic) transition should exist.

transition has a conjugate glass transition – the cluster-spin glass transition – which can be formed by doping non-magnetic defect (e.g. Zn) into a ferromagnetic system (e.g. CoFe_2O_4) [4], and the resultant cluster-spin glass is a frozen disordered arrangement of magnetic dipole clusters. Ferroelectric transition has a conjugate glass transition being relaxor transition; the latter can be formed by doping point defect (e.g. La^{3+}) into a normal ferroelectric system (e.g. BaTiO_3), and the resultant relaxor (e.g. La-BaTiO_3) is a frozen disordered arrangement of electric dipoles [5].

By the same reasoning, it is reasonable to expect a ‘strain glass transition’, which is the conjugate glass transition of a ferroelastic/martensitic transition. Such a strain glass transition should be the transition from a dynamically disordered lattice strain state (the paraelastic or the parent phase) to a frozen disordered strain state (strain glass). However, such a possibility has long remained obscure.

The possibility of strain glass was first suggested in 1990s by two notable theoretical studies of Kartha et al. [6,7] and Semenovskaya and Khachatryan [8]. These studies proposed that the premartensitic tweed is a strain glass (they used the term ‘spin glass’). Premartensitic tweed, a cross-hatched microstructure, is known to appear prior to martensitic transformation in various systems, but its nature has remained unclear [9,10]. Kartha et al. [6,7] and Semenovskaya and Khachatryan [8] concluded that point defects (or compositional disorder) play a key role in producing the strain glass; they also predicted that the tweed should possess non-ergodicity (or history dependence), which is a critical proof of a glass. However, there has been no experimental effort to verify their hypothesis.

In the present paper, we provide a critical experimental test of the above hypothesis on tweed being a strain glass. We selected two well-known alloys with premartensitic tweed or nano-domains prior to their martensitic transformation. The first is $\text{Ni}_{63}\text{Al}_{37}$, which shows highly anisotropic tweed [11,12]; the second is $\text{Ti}_{50}\text{Ni}_{47}\text{Fe}_3$, which shows isotropic nano-domain features due to its low elastic anisotropy [13,14]. We performed mechanical susceptibility measurement as a function of temperature to detect a possible glass transition. We also performed a field-cooling (FC) and zero-field-cooling (ZFC) experiment to detect the possible non-ergodicity of the tweed. Our results show that tweed does not possess the signatures expected of a frozen glass: there is no anomaly in mechanical susceptibility ($d\varepsilon/d\sigma$) and the tweed turns out to be ergodic. These results suggest that premartensitic tweed is not a strain glass.

Thus, two important questions arise. (i) Where is a true strain glass? (ii) If strain glass is something else, then what is premartensitic tweed and what is its relation to true strain glass? In this paper, we shall try to answer these two central questions.

In light of recent experimental finding of true strain glass in Ni-rich TiNi alloys [15–18], we shall show that strain glass appears in a defect-containing ferroelastic/martensitic system when defect concentration exceeds a critical value. It is a conjugate transition of a ferroelastic/martensitic transition, and it exhibits similar glass signatures as other glass transitions. We found that premartensitic tweed can be viewed as an ‘unfrozen state’ of strain glass. Finally, we shall discuss the microscopic origin of strain glass.

2. Experimental

In the present work, we used two well-known martensitic alloys with representative premartensitic tweed above their martensitic transformation. The first alloy is a $\text{Ni}_{63}\text{Ni}_{37}$ alloy, which represents a large class of martensitic alloys showing highly anisotropic premartensitic tweed. The second alloy is a $\text{Ti}_{50}\text{Ni}_{47}\text{Ni}_3$ alloy, which represents those martensitic alloys with almost isotropic tweed due to the low elastic anisotropy. Because these two tweed alloys are representative to all the premartensitic tweeds we encountered, our test for the possible glass signatures for these two alloys will enable us to make a general conclusion about whether or not tweed is a strain glass.

The $\text{Ni}_{63}\text{Ni}_{37}$ alloy was a single crystal cut into $30 \times 1.86 \times 1.26 \text{ mm}^3$. The sample was quenched from 1473 K into water to avoid diffusional decomposition. Its martensitic transformation starts at $M_s = 259.2 \text{ K}$. Tweed was known to appear a few tens of Kelvins above the M_s temperature in such an alloy [11]. The $\text{Ti}_{50}\text{Ni}_{47}\text{Fe}_3$ sample was a polycrystal cut into $30 \times 2.2 \times 0.8 \text{ mm}^3$. It was quenched from 1273 K into water to obtain a homogeneous composition. The martensitic transformation starts at $M_s = 263.4 \text{ K}$. In this alloy, the premartensitic tweed was found to appear as isotropic nano-domains over a temperature range a few tens of Kelvins above the M_s temperature [20].

To prove the existence of a glass, one needs to show the four essential signatures of a glass. (i) The existence of a glass transition from a disordered ergodic state (generic ‘liquid’ state) into a frozen disordered state (glass). Such a transition is characterized by a frequency-dependent peak in the susceptibility of the relevant order parameter, with the peak position obeying the Vogel–Fulcher relation. (ii) The non-ergodicity of the glass state. This can be tested by a FC/ZFC experiment to detect if the state of the system is history-dependent. In addition to the above two essential signatures, a glass should also (iii) have the same average (disordered) structure as the high temperature disordered phase and (iv) exhibit local or short-range order. These signatures have been found in all types of glasses [3,21].

To prove the premartensitic tweed is a strain glass, one needs to demonstrate the above-mentioned four signatures. Over the past decades, extensive diffractometry and TEM studies [11–13] have confirmed that the tweed has the same average structure as the high temperature parent phase, and it shows local lattice distortion (short-range strain ordering). These facts suggest that the tweed satisfies criteria (iii) and (iv) of a glass, which have been the experimental basis for the early suggestion of strain glass [6–8]. However, to prove the tweed is a strain glass, evidence for the most critical signatures (i) and (ii) is essential, but it is unclear whether or not the tweed possesses these two signatures.

To observe signature (i), we need to find a frequency-dependent peak in mechanical susceptibility – the compliance $d\varepsilon/d\sigma$; the peak temperature T_g (or the glass transition temperature) follows a Vogel–Fulcher relation with frequency. The appropriate test for this purpose is a dynamical mechanical measurement (DMA), which records the inverse of the mechanical susceptibility, the elastic modulus $d\sigma/d\varepsilon$ (together with the mechanical loss $\tan\delta$) as a function of both temperature and frequency. Single cantilever mode was used in our measurement and the frequency range was 0.2–20 Hz. The DMA used was a Q800 from TA Instruments.

To detect signature (ii), i.e. non-ergodicity, we need to locate a history dependence in the sample state, i.e. a difference between field-cooling (FC) and zero-field-cooling (ZFC) curves, as typically done for proving any type of glass [21]. Here, the ‘field’ is a small DC stress. We performed a static measurement with the DMA to achieve this. Under a small constant load of 30–40 MPa, we measured the sample strain as a function of temperature during heating of the sample with two different histories: ZFC and FC. For a strain glass, the ZFC and FC curves should deviate for $T < T_g$ (i.e. non-ergodic), and overlap for $T > T_g$ (i.e. ergodic), as being the case for any other glasses. Details on performing the ZFC and FC tests are available in [17].

3. Results

3.1. Determination of martensite start temperature

(M_s) for $Ni_{63}Al_{37}$ and $Ti_{50}Ni_{47}Fe_3$

Figure 2a and b show the DSC cooling curves for $Ni_{63}Al_{37}$ and $Ti_{50}Ni_{47}Fe_3$, respectively. The transition peak in the shaded regime represents the martensitic transformation from a B2 paraelastic/parent phase to a martensite (ferroelastic) phase. The former alloy shows a $M_s = 259.2$ K and the latter has a $M_s = 263.4$ K. From the literature, it is known that the premartensitic tweed or nano-domains are observed up to a few tens of Kelvin above the M_s [11–13].

3.2. Detection of possible glass transition in the premartensitic tweed temperature regime by DMA measurement

All types of glasses are formed from a dynamically disordered state (i.e. a generic ‘liquid’) through a freezing transition. As discussed in the previous section, such a freezing transition is characterized by an anomaly in the susceptibility of its order parameter, which has a frequency dispersion obeying the Vogel–Fulcher relation. To prove the tweed is a strain glass, we also need to identify that the tweed is formed by a freezing transition – the strain glass transition – from a dynamically strain-disordered state (the normal parent phase). As discussed in the previous section, the detection of a strain-freezing transition involved the mechanical susceptibility experiment, i.e. DMA experiment.

Figure 3a and b show the temperature and frequency dependence of the elastic modulus $d\sigma/d\varepsilon$ (the inverse of mechanical susceptibility $d\varepsilon/d\sigma$) of $Ni_{63}Al_{37}$ and $Ti_{50}Ni_{47}Fe_3$, respectively, measured by DMA. The loss is shown in the lower part of each figure. The anomaly in elastic modulus and loss in the shaded regime is due to the martensitic transformation, which is well known [24] and not of interest in this study. We are interested in the premartensitic tweed temperature regime, which is above the martensitic transformation temperature M_s . Because the temperature range of our DMA measurement is wider than 65 K above the M_s , any glass transition in the tweed regime should be detected as an anomaly in the elastic modulus. However, as can be seen in both Figure 3a and b, there is no modulus anomaly in the tweed regime nor is there any anomaly in the mechanical loss. This contrasts with the existence of a susceptibility anomaly in cluster-spin glass

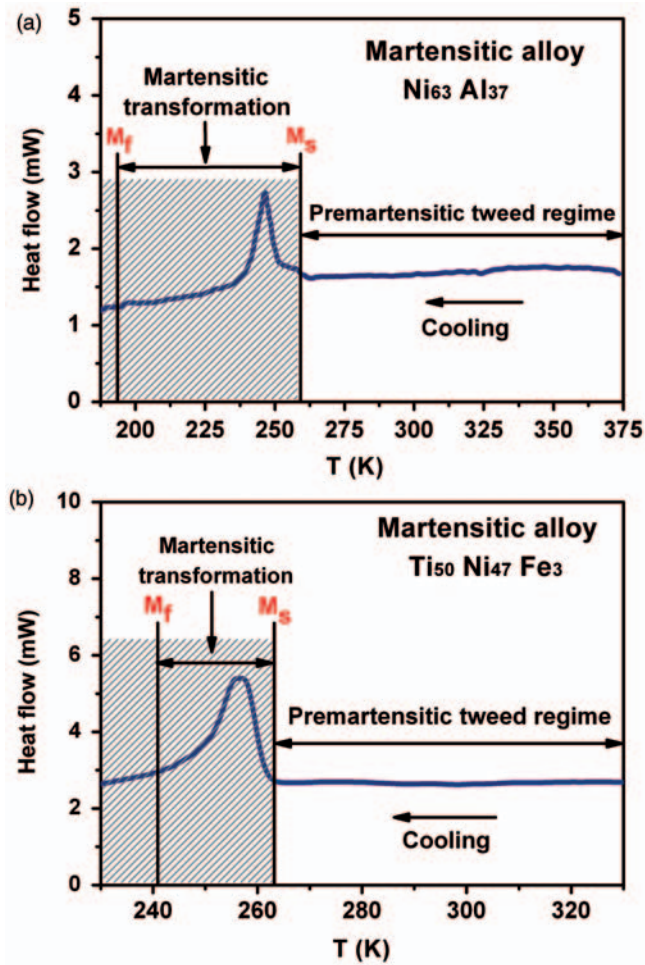


Figure 2. DSC cooling curves for $\text{Ni}_{63}\text{Al}_{37}$ and $\text{Ti}_{50}\text{Ni}_{47}\text{Fe}_3$. The premartensitic tweed appears above the shaded temperature regime. Martensitic transformation starts at M_s and finishes at M_f temperature.

195 (Figure 3c) [23] and ferroelectric relaxor (Figure 3d) [24]. Therefore, our AC mechanical susceptibility (modulus) experiment found no signature of a strain glass transition in the tweed regime.

3.3. Detection of possible non-ergodicity in the premartensitic tweed regime by a field-cooling/zero-field-cooling (FC/ZFC) experiment

200 As discussed in the previous section, crucial proof of a glass is to show its non-ergodicity, which is equivalent to a history dependence of the sample state. The standard test for history dependence is FC/ZFC experimentation. In such an experiment, a sample with two different prior histories (FC and ZFC) is tested during

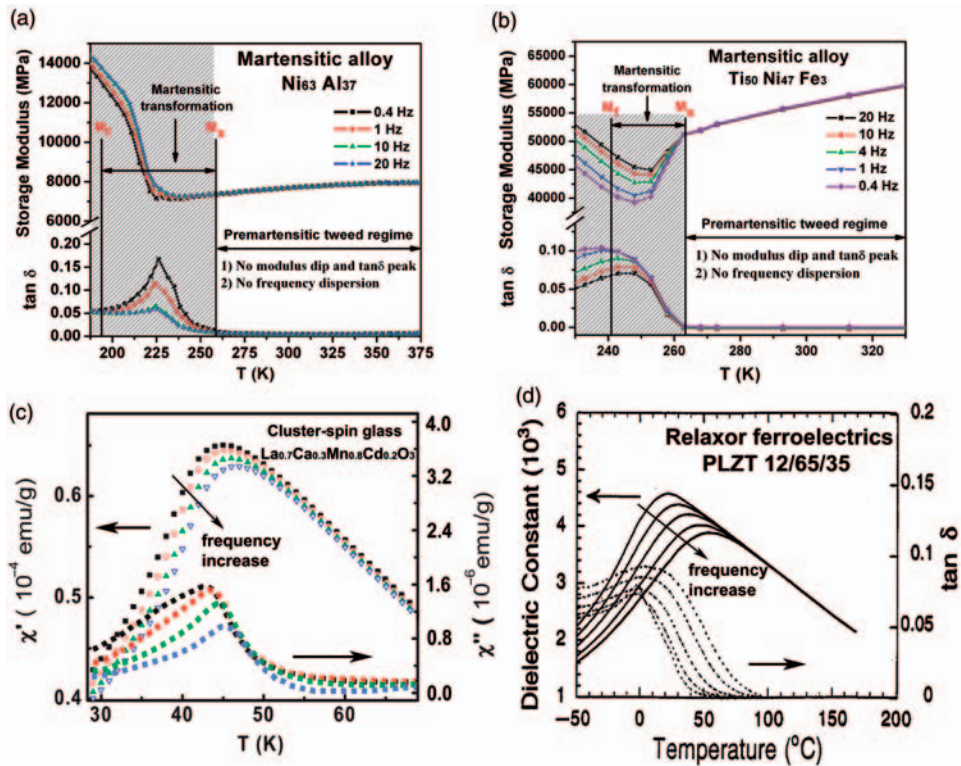


Figure 3. Absence of anomaly in mechanical modulus $d\sigma/d\varepsilon$ and loss ($\tan \delta$) in premartensitic tweed temperature regime for (a) $\text{Ni}_{63}\text{Al}_{37}$ and (b) $\text{Ti}_{50}\text{Ni}_{47}\text{Fe}_3$. This contrasts with the glass behavior of (c) cluster-spin glass (cited from [23]) and (d) ferroelectric relaxor (cited from [24]). The shaded area in (a) and (b) denotes the temperature regime where martensite forms; M_s and M_f denote martensite start and finish temperature, respectively.

warming from a frozen glass state (below T_g) to a dynamically disordered ‘liquid’ state (above T_g). If the FC and ZFC deviate below T_g , the system is said to be non-ergodic for $T < T_g$.

Figure 4a and b show FC/ZFC curves for $\text{Ni}_{63}\text{Al}_{37}$ and $\text{Ti}_{50}\text{Ni}_{47}\text{Fe}_3$, respectively, in their tweed temperature regime. It can be seen that within experimental uncertainty there is no deviation between the FC and ZFC curve for both samples in their tweed state. This contrasts with the characteristic deviation between FC and ZFC curves for well-known glasses, such as cluster-spin glass (Figure 4c) [25] and ferroelectric relaxor (Figure 4d) [26]. Therefore, the premartensitic tweed is not a strain glass because it is still essentially ergodic.

4. Discussion

4.1. Where is a true strain glass?

The experiments clearly show that the premartensitic tweed (or nano-domains) does not satisfy the essential features of a glass. In the first place, no glass transition

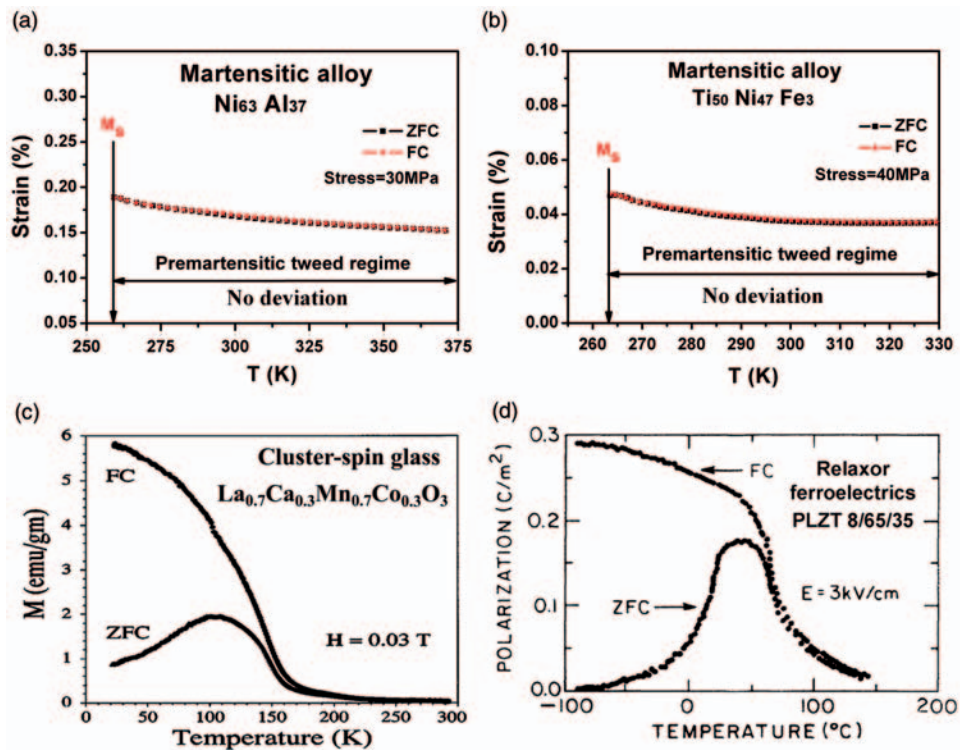


Figure 4. Absence of ergodicity breaking by field-cooling/zero-field-cooling (FC/ZFC) experiment for tweed in (a) Ni₆₃Al₃₇ and (b) Ti₅₀Ni₄₇Fe₃. The overlapping FC and ZFC curves for both tweed samples suggest an essentially ergodic behavior; this contrasts with the ergodicity breaking in (c) cluster-spin glass (cited from [25]) and (d) ferroelectric relaxor (cited from [26]) below their glass transition temperature (the peak temperature in the ZFC curve).

is found in the tweed temperature regime (Figure 3a, b). Secondly, the tweed is still essentially ergodic, as shown with the non-deviating FC/ZFC curves (Figure 4a, b).
 220 These two critical experiments show that the premartensitic tweed (or nano-domains) is not a strain glass and this conclusion remains true for the highly anisotropic tweed of Ni–Al alloys and nearly isotropic nano-domains of TiNi-based alloys.

Then, an intriguing question arises: if the premartensitic tweed (or nano-domains) is not a strain glass, where is a true strain glass? Actually, this question
 225 has been answered very recently by experimental studies on defect-containing ferroelastic/martensitic systems [15–19]. These studies have shown that true strain glass exists in defect-containing ferroelastic systems with defect concentrations above a critical value. The first example of strain glass was found in a well known martensitic system: binary Ti_{50-x}Ni_{50+x}. Strain glass appears when the standard
 230 martensitic alloy Ti₅₀Ni₅₀ is doped with excess Ni (as point defect) exceeding 1.3 mol%Ni (i.e. $x > 1.3$), as shown in Figure 5a. Doping defects (Ni here) in the normal martensitic system initially lower the martensitic transformation temperature, but when the doping level exceeds a critical concentration x_c , the martensitic

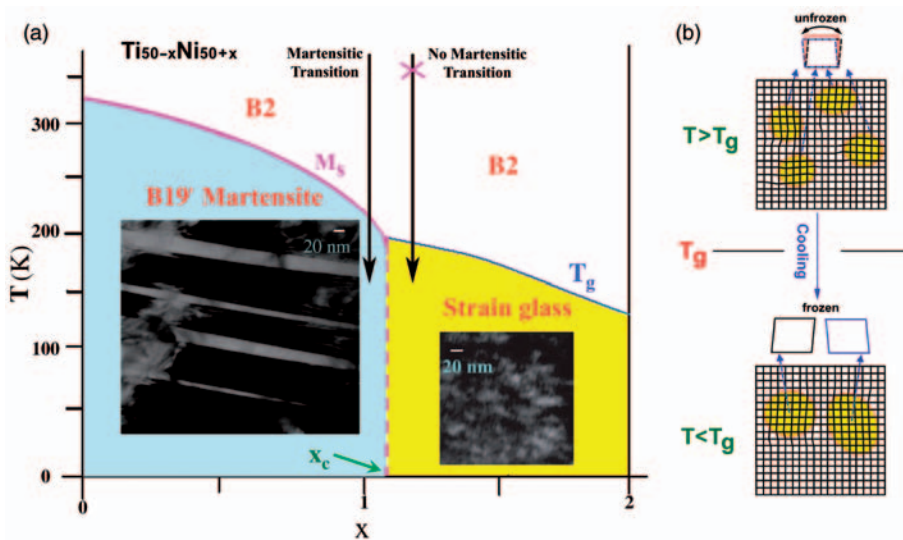


Figure 5. (a) Strain glass phase diagram of $Ti_{50-x}Ni_{50+x}$. Strain glass appears when defect concentration x exceeds 1.3. TEM micrographs showing the difference between normal martensite and strain glass in microstructure. Strain glass is characterized by random nano-sized strain domains. (b) Schematic illustration of strain glass transition. The strain domains in the unfrozen state (above glass transition T_g) are essentially dynamic (strain liquid); At $T < T_g$, these domains are frozen into a statically disordered state (frozen glass). This process is very similar to the freezing of gelatin water (defect-containing liquid) into a solid jelly.

transformation suddenly disappears and there is no sign of a structural transition,
 235 even down to 0 K [27]. However, seemingly non-transforming compositions turned
 out to undergo a strain glass transition, as proved by DMA [15,16] and FC/ZFC
 experiments [17].

The strain glass transition is schematically illustrated in Figure 5b. For $T > T_g$,
 the alloy is in an essentially 'strain liquid' state, with most nano-strain domains
 240 constantly flipping among their possible strain orientations; but the average
 structure is cubic. For $T < T_g$, the nano-strain domains are frozen into a statically
 disordered configuration, the strain glass; thus, the average structure still keeps the
 same cubic as for $T > T_g$. This explains why the frozen strain glass has the same
 average structure as the high temperature phase. The most important consequence
 245 of freezing is that the system loses ergodicity, which is a characteristic signature
 of a glass. Nevertheless, Figure 5b is an oversimplified picture of strain glass
 transition. As will be shown later, the strain liquid state can exhibit different degree
 of 'stickiness' depending on temperature and defect concentration. Strain liquid of
 different stickiness may display different transformation behavior.

250 Sarkar et al. [15] presented the first evidence for strain glass transition in a strain
 glass alloy $Ti_{48.5}Ni_{51.5}$ by DMA measurements. They discovered the existence of
 a frequency-dependent anomaly in both AC elastic modulus and loss at a freezing
 temperature T_g , which obeys the Vogel-Fulcher relation (Figure 6). This is strikingly
 similar to that of cluster-spin glass (Figure 3c) and ferroelectric relaxor (Figure 3d).

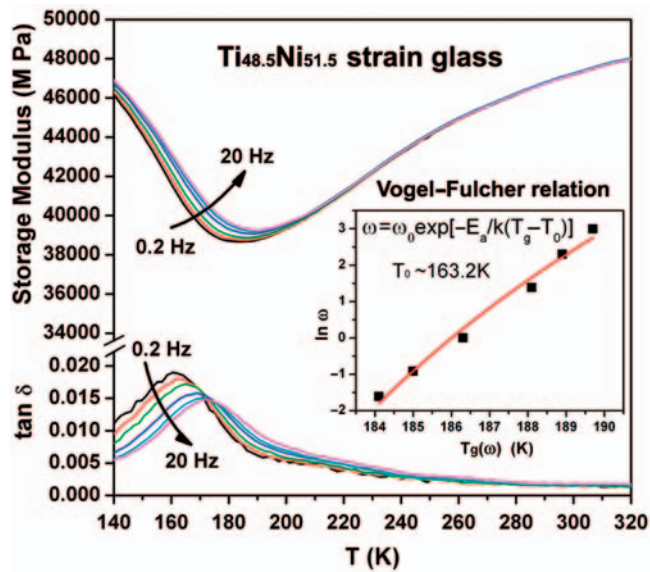


Figure 6. Evidence for strain glass transition in $\text{Ti}_{48.5}\text{Ni}_{51.5}$ by a DMA measurements, which measures the elastic modulus $d\sigma/d\varepsilon$ (top) and the inverse of the mechanical susceptibility, together with the loss $\tan \delta$ (bottom) as a function of temperature and frequency. The modulus anomaly (dip) corresponds to the glass transition temperature T_g , which is dependent on frequency ω . The inset shows the Vogel-Fulcher relation between T_g and ω .

255 Wang et al. [17] later proved via a FC/ZFC experiment that the strain glass transition indeed breaks ergodicity, as shown in Figure 7. The FC/ZFC curves of the strain glass are also striking similar to those of cluster-spin glass (Figure 4c) [25] and ferroelectric relaxor (Figure 4d) [26]. From the above critical experiments, strain glass is established as a fact. Its striking similarity to cluster-spin glass and relaxor
 260 enables the definition of a broader class of glass – ferroic glass [17] – because these three types of glasses are derived from three physically parallel ferroic transitions: ferroelastic, ferromagnetic and ferroelectric transitions.

We have found that similar strain glasses exist in a broad range of defect-containing ferroelastic/martensitic systems, such as TiNi-X [28], Ti-Pd-X [29], etc.,
 265 where X is an alloying element such as Fe, Cr, Mn, Co, V, etc. These results suggest that strain glass is a general phenomenon in defect-containing ferroelastic systems. It should be noted that recent computer simulations have also proved the existence of a glassy state with defect doping [14].

4.2. Relation between premartensitic tweed and strain glass

270 We will now try to answer the other key question: if the premartensitic tweed is not a strain glass, then what is it? Or equivalently, what is the relationship between tweed and strain glass? The clue for the answer to this important question comes from a comparison between the behavior of tweed and that of an unfrozen strain glass

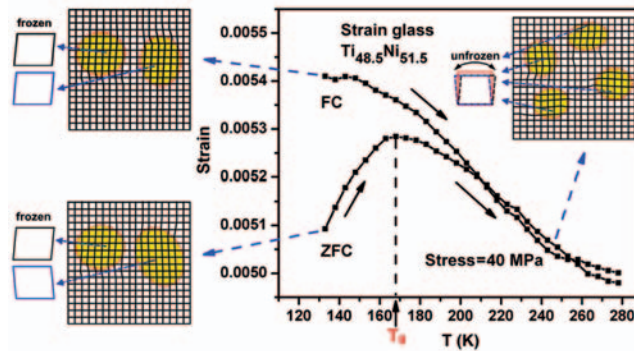


Figure 7. Evidence for ergodicity breaking in strain glass $\text{Ti}_{48.5}\text{Ni}_{51.5}$ for $T < T_g$, measured by a field-cooling/zero-field-cooling (FC/ZFC) experiment. The illustrations show the physical image of each state. At $T < T_g$, FC and ZFC create two different frozen strain domain configurations. ZFC creates completely random domains, whereas FC creates slightly aligned domains, as shown on the left-side illustrations. Such a history dependence (or non-ergodicity) of sample state causes the difference between FC and ZFC curves below T_g . At $T > T_g$, the domains are unfrozen and are constantly flipping among their possible variants; as a result, the prior history (FC or ZFC) will not affect its state and the FC and ZFC curves gradually overlap.

(i.e. the state for $T > T_g$ in Figure 5). Note that the premartensitic tweed for normal
275 martensitic compositions behaves very similarly to the unfrozen state of a strain
glass (i.e. $T > T_g$) in terms of dynamic behavior and FC/ZFC features, as shown in
Figures 8 and 9.

Figure 8a–c show a comparison of mechanical susceptibility (DMA) for two
280 types of premartensitic tweed ($\text{Ni}_{63}\text{Al}_{37}$ and $\text{Ti}_{50}\text{Ni}_{47}\text{Fe}_3$) and an unfrozen strain
glass $\text{Ti}_{48.5}\text{Ni}_{51.5}$ (for $T > T_g$). It was found that the tweed of the two martensitic
alloys (Figure 8a, b) behaves essentially the same as the unfrozen strain glass
(i.e. $T > T_g$). They all show an elastic softening with lowering temperature, which has
no appreciable frequency dispersion, but the unfrozen strain glass shows a slight
frequency dispersion in the vicinity of its freezing temperature T_g . Figure 9a–c show
285 a comparison of the FC/ZFC curves for these three samples. It was found that both
the premartensitic tweed ($\text{Ni}_{63}\text{Al}_{37}$ and $\text{Ti}_{50}\text{Ni}_{47}\text{Fe}_3$) and the unfrozen strain glass
 $\text{Ti}_{48.5}\text{Ni}_{51.5}$ (for $T > T_g$) are essentially ergodic, but the unfrozen strain glass shows
a slight non-ergodicity in the vicinity of T_g . Such a slight non-ergodicity at $T \rightarrow T_g$
corresponds to the same temperature range in Figure 8c showing frequency
dispersion. Therefore, Figures 8 and 9 suggest that the premartensitic tweed has the
290 same physical nature as an unfrozen strain glass, except that the latter shows slight
non-ergodicity when approaching T_g . Such a small difference will be explained later.

From the above finding that the premartensitic tweed is equivalent to an
unfrozen strain glass, we can draw a generic strain glass phase diagram as shown in
295 Figure 10, which shows the relationship between premartensitic tweed, strain glass,
normal parent phase and martensite. The physical picture of these states is as
follows. For a strain glass composition ($x > x_c$), the system transforms from an
unfrozen strain glass into a frozen strain glass at T_g . During this process, from very

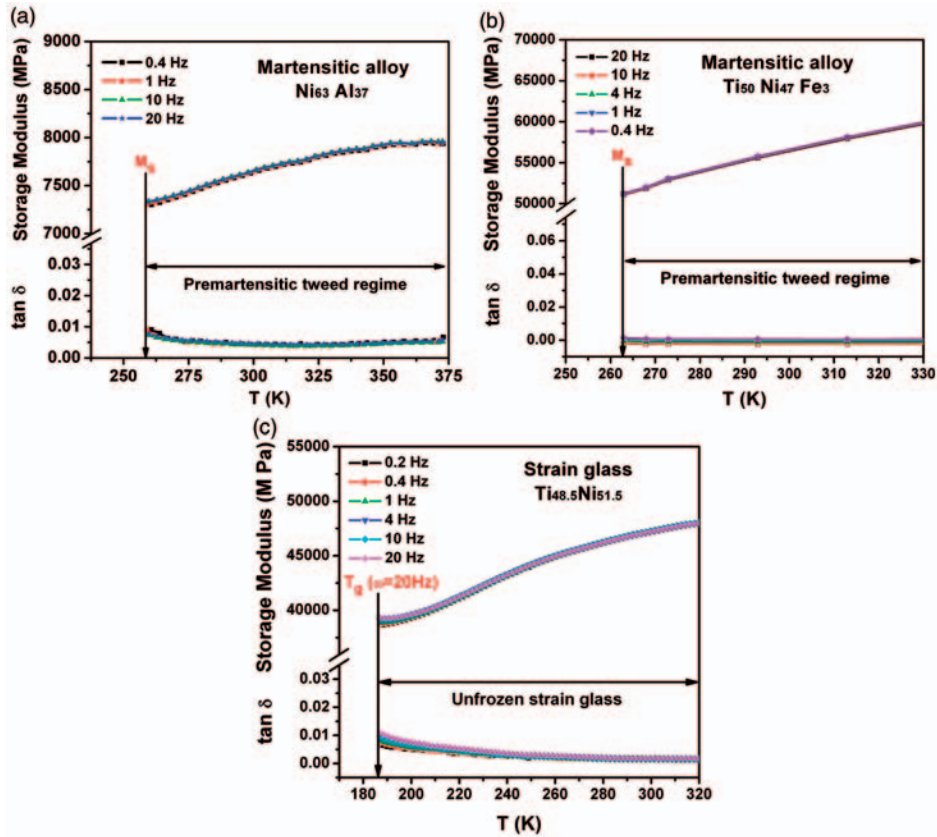


Figure 8. Similarity in AC behavior of premartensitic tweed (at $T > M_s$) of (a) $Ni_{63}Al_{37}$ and (b) $Ti_{50}Ni_{47}Fe_3$ with (c) an unfrozen strain glass $Ti_{48.5}Ni_{51.5}$ (for $T > T_g$) measured by DMA. In each figure, the temperature dependence of the elastic modulus $d\sigma/d\varepsilon$ (inverse of mechanical susceptibility) is shown in the top part, and that of the loss ($\tan \delta$) is shown in the bottom part. The tweed in both $Ni_{63}Al_{37}$ and $Ti_{50}Ni_{47}Fe_3$ behaves like an unfrozen strain glass $Ti_{48.5}Ni_{51.5}$ (for $T > T_g$), except that the latter shows slight frequency dispersion in the vicinity of T_g .

high temperature ($T \gg T_g$) to low temperature, the system changes gradually from a
 300 'strain liquid' (for $T \gg T_g$) to a 'less-sticky strain liquid' (for $T > T_g$), and to a 'sticky
 strain liquid' (for $T \rightarrow T_g$) before freezing into a frozen strain glass at T_g , as shown in
 Figure 10. It is similar to gelatin water increasing its stickiness during cooling and
 eventually freezing into a solid jelly. For a strain glass system, the stickiness, i.e. slow
 305 mechanical response, is caused by the existence of quasi-static strain domains in the
 otherwise ideal strain liquid. With lowering temperature, the quasi-static domains
 increases in number and size, thus making the unfrozen strain glass progressively
 stickier, until all the domains become static and frozen at freezing temperature T_g .
 The quasi-static domains are imaged as nano-domains or tweed under TEM,
 and they have been found to grow with lowering temperature and finally freeze
 310 around T_g [15]. It should be noted that strain liquid and less-sticky liquid are

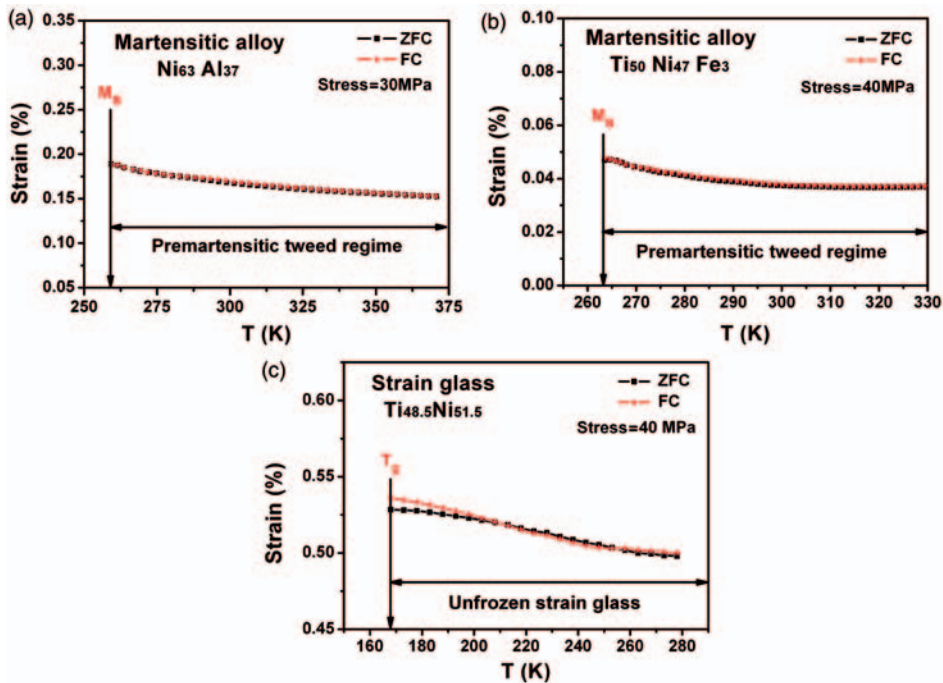


Figure 9. Comparison of field-cooling/zero-field-cooling (FC/ZFC) curve of the premartensitic tweed of (a) $\text{Ni}_{63}\text{Al}_{37}$ and (b) $\text{Ti}_{50}\text{Ni}_{47}\text{Fe}_3$ with (c) an unfrozen strain glass $\text{Ti}_{48.5}\text{Ni}_{51.5}$ (for $T > T_g$). The tweed in both $\text{Ni}_{63}\text{Al}_{37}$ and $\text{Ti}_{50}\text{Ni}_{47}\text{Fe}_3$ shows similar ergodic behavior as the unfrozen strain glass $\text{Ti}_{48.5}\text{Ni}_{51.5}$, except that the latter has a slight non-ergodicity in the vicinity of T_g .

essentially ergodic as the quasi-static nano-domains are few in number and small in size. This is consistent with the observation in Figures 8c and 9c that unfrozen strain glass shows ergodic behavior at temperatures not close to T_g . For a sticky strain glass (i.e. $T \rightarrow T_g$), a small non-ergodicity exists, as shown in Figures 8c and 9c, in the vicinity of T_g . For a frozen glass ($T < T_g$), a large non-ergodicity appears, as shown in Figure 7.

For a premartensitic tweed system (with low defect concentration $x < x_c$), the picture is essentially the same as of an unfrozen strain glass ($x > x_c$). At high temperature, the system is in a strain liquid state and with lowering temperature the strain liquid becomes progressively stickier. However, unlike unfrozen strain glass, this strain liquid cannot become sufficiently sticky to be able to freeze into a strain glass due to the lower defect concentration. Instead, it undergoes a strain ordering at low temperature, i.e. becoming a martensite. This situation is similar to that of doping a low concentration of gelatin into water, which can make the liquid stickier but will not suppress the crystallization transition. It should be noted that this less-sticky strain liquid can still form quasi-static strain domains (or tweed), as observed by TEM [11,13], but their effect on non-ergodicity is too small to be detected by conventional AC or FC/ZFC experiments. This is why the static premartensitic tweed coincides with experimentally observed ergodic

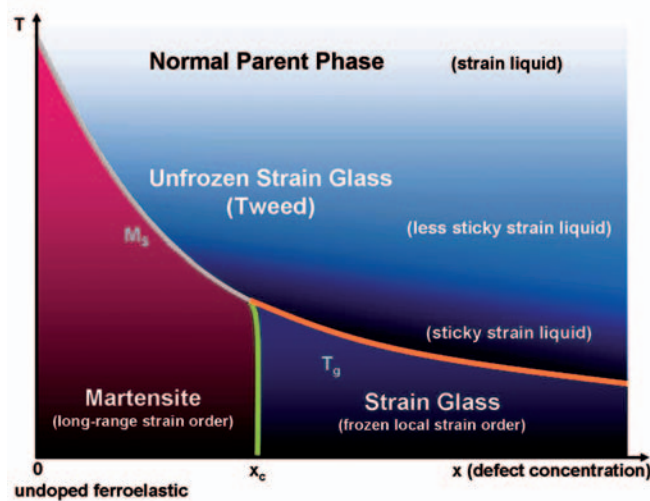


Figure 10. Relationship between strain glass, tweed, normal parent phase and martensite. Strain glass appears only when defect concentration x exceeds a critical value x_c . For $x > x_c$, the system undergoes a transition at T_g from an unfrozen strain glass to a strain glass. In the unfrozen glass state, during cooling from high temperature, the system evolves from a strain liquid (the normal parent phase) to a less sticky strain liquid, and finally to a sticky strain liquid, before freezing into a strain glass at T_g . For $x < x_c$, during cooling from high temperature, the system changes from a strain liquid (the normal parent phase) to a less-sticky strain liquid state, and eventually orders into a normal martensite. In the less-sticky and sticky strain liquid states, there exist quasi-static strain domains, which appear as a tweed pattern or in the form of nano-domains (depending on elastic anisotropy). For the undoped ferroelastic ($x=0$), the strain liquid does not become sticky, as there are no point defects; thus, such a strain liquid transforms directly into a martensite, without passing a sticky state – the tweed.

330 behavior (Figures 8a, b and 9a, b). In a word, the premartensitic tweed is nothing
but an unfrozen strain glass with ‘less-stickiness’ due to low defect concentration.
Such a less-sticky strain liquid transforms into martensite rather than into strain
glass, as shown in Figure 10.

335 In the extreme case of having no defects (i.e. $x=0$ in Figure 10), the high
temperature strain liquid will not become ‘sticky’ with lowering temperature. Thus,
we cannot observe a premartensitic tweed above the martensitic transformation
temperature. Therefore, Figure 10 confirms our understanding for ideal martensitic
transformation without defects, the formation of tweed at low defect doping prior to
martensitic transformation, the suppression of martensitic transformation and the
340 formation of strain glass at high defect doping.

Based on Figure 10, we can predict a new effect for premartensitic tweed. For a
premartensitic tweed system that undergoes a normal martensitic transformation,
if we can somehow suppress the martensitic transformation by applying a suitable
external influence (pressure, stress, or other field), we predict that the premartensitic
345 tweed will eventually freeze into a strain glass at low temperature. Verification of this
interesting prediction will be a crucial test of the key physical picture discussed
in Figure 10.

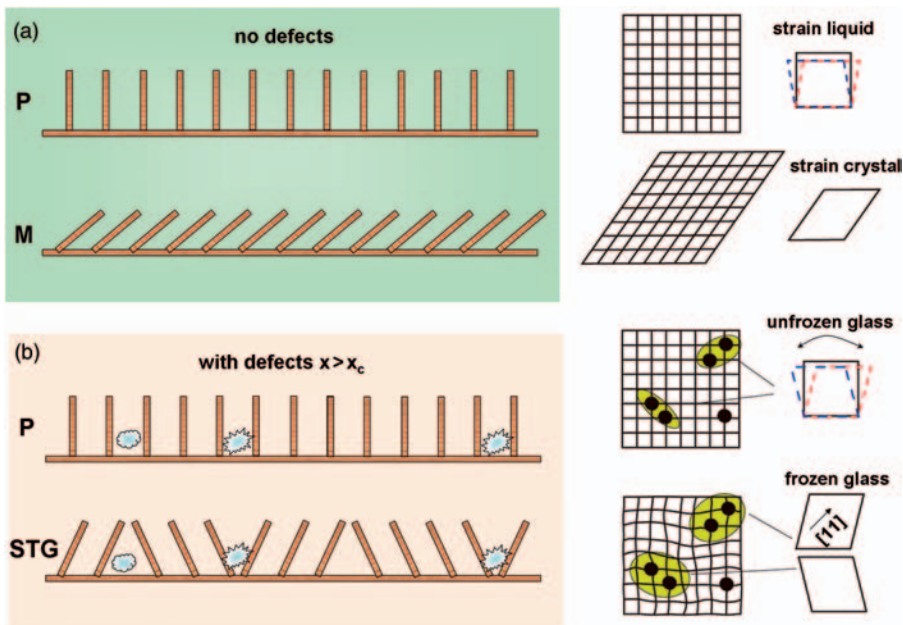


Figure 11. Microscopic origin of strain glass: destruction of long-range strain ordering by point defects. (a) Normal martensitic transformation (long-range strain ordering) in the absence of defects. The parent state (P) and martensite state (M) are an analogy to the two states of a domino array shown on the left. (b) Strain glass transition (frozen short-range ordering) appears at high defect concentration. This is analogous to the situation where the introduction of many stones (defects) into the domino array will destroy the long-range ordering and, instead, a short-range ordered state is formed, as shown on the left side.

4.3. Microscopic origin of strain glass: the domino model

Let us now discuss the microscopic origin of strain glass formation at high defect concentration. A phenomenological explanation based on energy landscapes has been given in our recent paper [18]. Here, we provide a simple microscopic picture that can be easily understood by making an analogy to the behavior of a domino array.

Figure 11a shows the analogy of a normal martensitic transformation in a pure system with the long-range propagation (ordering) of identical domino blocks. Clearly, the system can undergo a long-range strain ordering, as there are no defects to destroy the long-range ordering. Figure 11b shows the situation with sufficient defect concentration. The 'defects' in the domino array can be considered as irregular stones placed randomly in the array. Each stone has its own local preference for the way that the nearby blocks should fall, but different stones have different preferences. As a result, when the dominos fall they cannot fall in a long-range ordered way, as in the case of no defect; instead, a locally ordered but long-range disordered pattern appears, as shown on the left side of Figure 11b. Strain glass formation stems from the same origin. Point defects (most probably defect pairs) create local lattice distortion that favors a particular strain domain for each defect pair; but, as the defect pairs are randomly distributed, the system can order only into

a locally ordered but long-range disordered state, as shown on the right side of Figure 11b. This is analogous to the ‘domino array with stones’ case. We believe Figure 11 reveals the essential physics of a strain glass, and may be a starting point for a quantitative theory of strain glass. A possible approach may be the extension of earlier models of spin glass (e.g. the Sherrington–Kirkpatrick model [30,31]) to reflect the physical picture of Figure 11. Another approach may be based on a Landau–Ginzburg type model (like that used by Khachatryan [32], Lloveras et al. [14] and Shenoy et al. [33]) with the introduction of coupling between the strain order parameter and the random field created by point defects.

5. Conclusions

- (1) Premartensitic tweed is not a strain glass because it does not show the essential features of a glass.
- (2) True strain glass occurs in a ferroelastic system when defect concentration exceeds a critical value. For such compositions, the strain glass undergoes a transition from an unfrozen glass into a frozen glass around the freezing temperature T_g . The unfrozen state ($T > T_g$) of strain glass can be viewed as a strain liquid with stickiness increasing continuously with cooling to T_g , from a normal strain liquid to a less-sticky strain liquid, and then to a sticky strain liquid. The ‘stickiness’ is caused by the existence of quasi-static strain domains in the otherwise dynamic liquid. These quasi-static domains appear in the form of a tweed pattern or nano-domains depending on the elastic anisotropy of the system.
- (3) Relationship between premartensitic tweed and strain glass: premartensitic tweed corresponds to an unfrozen strain glass with less stickiness due to low defect concentration. It transforms into martensite rather than to a frozen strain glass upon cooling. Strain glass exists only at high defect concentration, where the unfrozen strain glass can become ‘very sticky’ during cooling and, thus, eventually freezes into a frozen strain glass below T_g instead of transforming into a martensite.
- (4) A generic phase diagram of strain glass as a function of defect concentration is proposed, which explains the relation between normal parent phase (paraelastic phase), premartensitic tweed, martensite and strain glass.
- (5) Microscopic origin of strain glass: random point defects create random local stresses/strains that destroy the long-range ordering of strains.

Acknowledgements

The authors thank A. Saxena, T. Lookman and Y.Z. for stimulating discussions. Y. Wang acknowledges the financial support under a JSPS fellowship.

References

- [1] G. Careri, *Order and Disorder in Matter*, Addison-Wesley, Reading, MA, 1984.
- [2] V.K. Wadhawan, *Introduction to Ferrous Materials*, Gordon and Breach, Amsterdam, 2000.
- 410 [3] K. Binder and W. Kob, *Glassy Materials and Disordered Solids*, World Scientific, London, 2005.
- [4] R.N. Bhowmik and R. Ranganathan, *J. Magn. Magn. Mater.* 248 (2002) p.101.
- [5] R.T. Zhang, J.F. Li and D. Vieland, *J. Am. Ceram. Soc.* 87 (2004) p.864.
- [6] S. Kartha, T. Castan, J.A. Krumhansl and J.P. Sethna, *Phys. Rev. Lett.* 67 (1991) p.3630.
- 415 [7] S. Kartha, J.A. Krumhansl, J.A. Sethna and L.K. Wickham, *Phys. Rev. B* 52 (1995) p.803.
- [8] S. Semenovskaya and A.G. Khachatryan, *Acta Mater.* 45 (1997) p.4367.
- [9] A. Planes and L. Manosa, *Solid State Phys.* 55 (2001) p.159.
- [10] K. Otsuka and X. Ren, *Prog. Mater. Sci.* 50 (2005) p.511.
- 420 [11] S.M. Shapiro, J.Z. Lareze, Y. Noda, S.C. Moss and L.E. Tanner, *Phys. Rev. Lett.* 57 (1986) p.3199.
- [12] D. Schryvers and L. Tanner, *Ultramicroscopy* 32 (1990) p.241.
- [13] Y. Murakami, H. Shibuya and D. Shindo, *J. Microsc.* 203 (2000) p.22.
- [14] P. Lloveras, T. Castan, M. Porta, A. Planes and A. Saxena, *Phys. Rev. Lett.* 100 (2008) p.165707.
- 425 [15] S. Sarkar, X. Ren and K. Otsuka, *Phys. Rev. Lett.* 95 (2005) p.205702.
- [16] Y. Wang, X. Ren and K. Otsuka, *Phys. Rev. Lett.* 97 (2006) p.225703.
- [17] Y. Wang, X. Ren, K. Otsuka and A. Saxena, *Phys. Rev. B.* 76 (2007) p.132201.
- [18] Y. Wang, X. Ren, K. Otsuka and A. Saxena, *Acta Mater.* 56 (2008) p.2885.
- 430 [19] Y. Wang, X. Ren and K. Otsuka, *Mater. Sci. Forum.* 583 (2008) p.67.
- [20] Y. Murakami and D. Shindo, *Phil. Mag. Lett.* 81 (2001) p.631.
- [21] J.A. Mydosh, *Spin Glasses*, Taylor & Francis, London, 1993.
- [22] G.L. Fan, Y.M. Zhou, K. Otsuka and X.B. Ren, *Appl. Phys. Lett.* 89 (2006) p.161902.
- [23] S. Karmakar, S. Taran and B.K. Chaudhuri, *Phys. Rev. B* 74 (2006) p.104407.
- 435 [24] Q. Tan, J.F. Li and D. Viehland, *J. Appl. Phys.* 88 (2000) p.3433.
- [25] N. Gayathri, A.K. Raychaudhuri, S.K. Tiwary, R. Gundakaram, A. Arulraj and CNR Rao, *Phys. Rev. B* 56 (1997) p.1345.
- [26] D. Viehland, *Phys. Rev. B* 46 (1992) p.8013.
- 440 [27] T. Kakeshita, T. Fukuda, H. Tetsukawa, T. Saburi, K. Kindo, T. Takeuchi, M. Honda, S. Endo, T. Taniguchi and Y. Miyako, *Jpn J. Appl. Phys.* 37 (1998) p.2535.
- [28] D. Wang et al. (2008), to be published.
- [29] Y.M. Zhou et al. (2008), to be published.
- [30] D. Sherrington and S. Kirkpatrick, *Phys. Rev. Lett.* 35 (1975) p.1792.
- [31] D. Sherrington and S. Kirkpatrick, *Phys. Rev. B* 17 (1978) p.4384.
- 445 [32] A.G. Khachatryan, *Theory of Structural Transformation in Solid [M]*, Wiley, New York, 1983.
- [33] S.R. Shenoy, T. Lookman, A. Saxena and A.R. Bishop, *Phys. Rev. B* 60 (1999) p.12537.